

Improved performance of MoS_2 FET by *in situ* NH_3 doping in ALD Al_2O_3 dielectric

Xiaoting Sun(孙小婷), Yadong Zhang(张亚东), Kunpeng Jia(贾昆鹏), Guoliang Tian(田国良), Jiahan Yu(余嘉晗), Jinjuan Xiang(项金娟), Ruixia Yang(杨瑞霞), Zhenhua Wu(吴振华), and Huaxiang Yin(殷华湘)

Citation: Chin. Phys. B, 2022, 31 (**7**): 077701. DOI: 10.1088/1674-1056/ac3bab
Journal homepage: http://cpb.iphy.ac.cn; http://iopscience.iop.org/cpb

What follows is a list of articles you may be interested in

Oxygen vacancy control of electrical, optical, and magnetic properties of $Fe_{0.05}Ti_{0.95}O_2$ epitaxial films

Qing-Tao Xia(夏清涛), Zhao-Hui Li(李召辉), Le-Qing Zhang(张乐清), Feng-Ling Zhang(张凤玲), Xiang-Kun Li(李祥琨), Heng-Jun Liu(刘恒均), Fang-Chao Gu(顾方超), Tao Zhang(张涛), Qiang Li(李强), and Qing-Hao Li(李庆浩)
Chin. Phys. B, 2021, 30 (**11**): 117701. DOI: 10.1088/1674-1056/ac078e

Synergistic effects of electrical and optical excitations on TiO_2 resistive device

Qi Mao(毛奇), Wei-Jian Lin(林伟坚), Ke-Jian Zhu(朱科建), Yang Meng(孟洋), Hong-Wu Zhao(赵宏武)
Chin. Phys. B, 2017, 26 (**8**): 087702. DOI: 10.1088/1674-1056/26/8/087702

Recent progress of the native defects and p-type doping of zinc oxide

Kun Tang(汤琨), Shu-Lin Gu(顾书林), Jian-Dong Ye(叶建东), Shun-Ming Zhu(朱顺明), Rong Zhang(张荣), You-Dou Zheng(郑有炓)
Chin. Phys. B, 2017, 26 (**4**): 047702. DOI: 10.1088/1674-1056/26/4/047702

Interfacial and electrical properties of HfAlO/GaSb metal-oxide-semiconductor capacitors with sulfur passivation

Tan Zhen, Zhao Lian-Feng, Wang Jing, Xu Jun
Chin. Phys. B, 2014, 23 (**1**): 017701. DOI: 10.1088/1674-1056/23/1/017701

Effects of O_2/Ar ratio and annealing temperature on electrical properties of Ta_2O_5 film prepared by magnetron sputtering

Huang Shi-Hua, Cheng Pei-Hong, Chen Yong-Yue
Chin. Phys. B, 2013, 22 (**2**): 027701. DOI: 10.1088/1674-1056/22/2/027701

Improved performance of MoS_2 FET by *in situ* NH_3 doping in ALD Al_2O_3 dielectric

Xiaoting Sun(孙小婷)[1,2], Yadong Zhang(张亚东)[2], Kunpeng Jia(贾昆鹏)[2], Guoliang Tian(田国良)[2,3], Jiahan Yu(余嘉晗)[2], Jinjuan Xiang(项金娟)[2], Ruixia Yang(杨瑞霞)[1], Zhenhua Wu(吴振华)[2,3,†], and Huaxiang Yin(殷华湘)[2,3,‡]

[1] *School of Information Engineering, Hebei University of Technology, Tianjin* 300401, *China*
[2] *Key Laboratory of Microelectronics Device and Integrated Technology, Institute of Microelectronics Chinese Academy of Sciences, Beijing* 100029, *China*
[3] *University of Chinese Academy of Sciences, Beijing* 100049, *China*

(Received 25 September 2021; revised manuscript received 14 November 2021; accepted manuscript online 20 November 2021)

Since defects such as traps and oxygen vacancies exist in dielectrics, it is difficult to fabricate a high-performance MoS_2 field-effect transistor (FET) using atomic layer deposition (ALD) Al_2O_3 as the gate dielectric layer. In this paper, NH_3 *in situ* doping, a process treatment approach during ALD growth of Al_2O_3, is used to decrease these defects for better device characteristics. MoS_2 FET has been well fabricated with this technique and the effect of different NH_3 *in situ* doping sequences in the growth cycle has been investigated in detail. Compared with counterparts, those devices with NH_3 *in situ* doping demonstrate obvious performance enhancements: I_{on}/I_{off} is improved by one order of magnitude, from 1.33×10^5 to 3.56×10^6, the threshold voltage shifts from -0.74 V to -0.12 V and a small subthreshold swing of 105 mV/dec is achieved. The improved MoS_2 FET performance is attributed to nitrogen doping by the introduction of NH_3 during the Al_2O_3 ALD growth process, which leads to a reduction in the surface roughness of the dielectric layer and the repair of oxygen vacancies in the Al_2O_3 layer. Furthermore, the MoS_2 FET processed by *in situ* NH_3 doping after the Al and O precursor filling cycles demonstrates the best performance; this may be because the final NH_3 doping after film growth restores more oxygen vacancies to screen more charge scattering in the MoS_2 channel. The reported method provides a promising way to reduce charge scattering in carrier transport for high-performance MoS_2 devices.

Keywords: MoS_2, Al_2O_3 dielectric, NH_3 *in-situ* doping, oxygen vacancy

PACS: 77.22.Ch, 85.30.–z, 81.07.–b, 74.62.Dh **DOI:** 10.1088/1674-1056/ac3bab

1. Introduction

In 2004, the discovery of graphene attracted much research attention to two-dimensional (2D) materials.[1] Graphene has an ultra-high mobility of up to 2×10^5 $cm^2 \cdot V^{-1} \cdot s^{-1}$,[2] but its gapless nature limits its applications in the field of electronic transistors. Alternative transition metal dichalcogenides (TMDs) with atomic thickness and a tunable bandgap can overcome the shortcomings of graphene and demonstrate unique optical and electrical properties.[3–6] Molybdenum disulfide (MoS_2), one of the most widely studied TMDs, shows a variety of bandgaps from 1.2 eV to 1.9 eV with films from bulk to monolayer.[7] The fabricated MoS_2 field-effect transistors (FETs) show high carrier mobility,[8] high on–off ratios[9] and excellent subthreshold swing,[10] and have great possibilities for application in a variety of electronic devices, such as sensors,[11] photodetectors,[12] and logic devices.[13]

Theoretically, the intrinsic mobility of MoS_2 FETs can reach 410 $cm^2 \cdot V^{-1} \cdot s^{-1}$,[14] but in practice the reported mobility is far less than that. There are many scattering mechanisms in the devices, including charged impurity (CI) scattering, one of the most important factors that degrades mobility.[15] For a back-gate structure FET, the interface states between the 2D channel material and the gate dielectric can be improved by using a high-κ dielectric instead of SiO_2 to provide a special passivation process for effectively screening CI scattering. Many experimental results also show that MoS_2 FETs with high-κ gate dielectrics, such as HfO_2,[16] ZrO_2,[17] and Al_2O_3,[18] exhibit good electrical performance. However, the oxygen vacancies and dangling bonds distributed on the surface of high-κ dielectrics lead to the interface-state density of dielectrics/MoS_2 reaching 10^{11}–10^{12} $cm^{-1} \cdot eV^{-1}$.[19] Recently, much effort has been made to decrease the interfacial defects, such as various plasma treatments (O_2, N_2, NH_3, and CF_4/O_2),[20–23] rapid thermal annealing (RTA)[24,25] and dielectric-mediated doping[26] after the deposition of high-κ films. Proper nitrogen doping into the dielectrics during the deposition process supplies an effective way to improve the quality of the dielectrics.[27] Compared with treatments after growth, *in situ* doping is easier and effective. However, no research has yet been reported on *in situ* NH_3 doped Al_2O_3 as a gate dielectric in MoS_2 FETs. In this work, MoS_2 FETs with NH_3 doped atomic layer deposition (ALD) Al_2O_3 are systemically explored. Through x-ray photoelectron spectroscopy (XPS) and atomic force microscopy (AFM) characterization and electrical tests, the effects of different sequences

†Corresponding author. E-mail: wuzhenhua@ime.ac.cn
‡Corresponding author. E-mail: yinhuangxiang@ime.ac.cn

© 2022 Chinese Physical Society and IOP Publishing Ltd

of NH_3 doping into the gate dielectric on device performance are investigated. The results show that MoS_2 FETs with ALD Al_2O_3 doped with NH_3 during the final stages demonstrate the best performance; this is consistent with the results of dielectric analysis.

2. Experiments

In the FET experiments, a heavily doped p++ Si (100) 8inch wafer was used as the back gate. The gate dielectric was formed from an ALD Al_2O_3 thin film grown at 300 °C using trimethylaluminum (TMA; $Al(CH)_3$) and H_2O as Al and oxygen precursors, respectively. Firstly, TMA vapors are pulsed into the chamber and adsorb on the substrate surface, followed by pulsing of N_2 into the chamber to purge the unabsorbed TMA. Then H_2O vapors are pulsed to react with TMA to generate Al_2O_3 and other by-products. At the end of the cycle, N_2 is pumped in to remove excess gas and any other gases produced. The control of the film thickness is achieved by changing the number of cycles. In this work, the growth rate of the undoped Al_2O_3 film is 1.05 Å/cycle and a 20 nm thick film is grown after 190 cycles. To realize nitrogen doping in the Al_2O_3 dielectric layer, different sequences for introducing NH_3 into the growth cycle were designed in this experiment, as shown in Fig. 1. The growth sequence TMA–N_2–H_2O–N_2–NH_3–N_2 is called AlON (0.89 Å/cycle, 224 cycles for 20 nm) and the sequence TMA–N_2–NH_3–N_2–H_2O–N_2 is called AlNO (1.05 Å/cycle, 190 cycles for 20 nm).

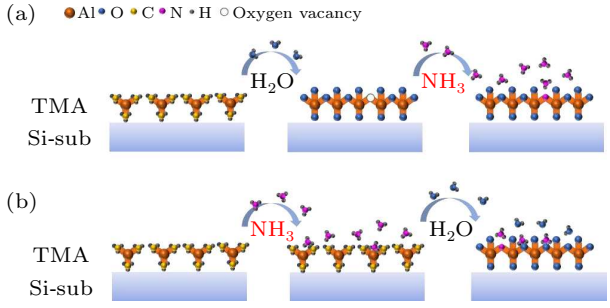


Fig. 1. Schematic diagrams of one cycle with different NH_3 doping sequences.

The MoS_2 flake channel material was mechanically exfoliated from bulk MoS_2 crystal (purchased from Six Carbon Technology, Shenzhen) using scotch tape and then transferred onto the target substrate by PDMS. Next, lithography with a negative polymer resist was used to define the source/drain region. Then, the metal electrode (Ti/Au = 10/40 nm) was deposited by electron beam evaporation, and the metal was stripped by lift-off to form a separate metal electrode.

Figure 2(a) is a schematic diagram of a few-layer MoS_2 FET with a 20 nm Al_2O_3 gate dielectric and Ti/Au electrodes. The prepared MoS_2 FET is shown in Fig. 2(b), and the length and width of the channel are 3 μm and 10.86 μm, respectively. The thickness of MoS_2 measured by AFM is 6 nm, as shown in Fig. 2(c). Figure 2(d) shows the Raman spectra of the MoS_2 flake and the Raman shift between the E^1_{2g} peak (384 cm^{-1}) and the A_{1g} peak (408 cm^{-1}) is 24 cm^{-1}.

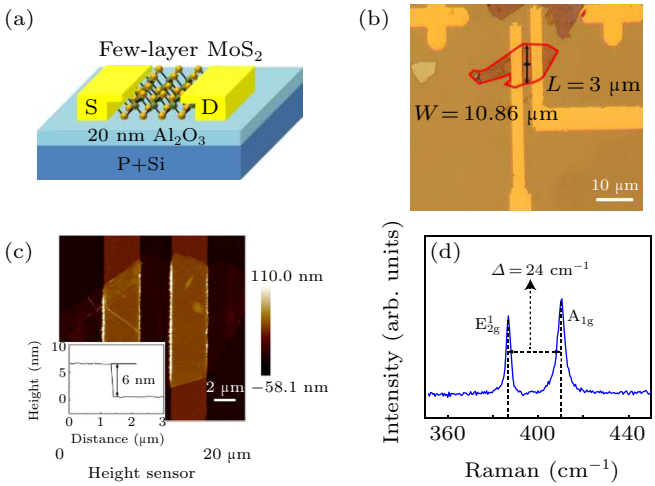


Fig. 2. (a) Schematic of a few-layer MoS_2 FET with a 20 nm Al_2O_3 gate dielectric and Ti/Au electrodes. (b) Optical photograph of the prepared MoS_2 transistor. (c) AFM image of the MoS_2 transistor with the inset showing the thickness of the MoS_2 flake measured by AFM. (d) Raman spectra of MoS_2 flake.

The high-frequency (1 MHz) capacitance–voltage (C–V) curves and the electrical characteristics of MoS_2 FETs were measured using a Keithley 4200-SCS and an Agilent 4156C, respectively, at room temperature in an atmospheric environment.

3. Results and discussion

The influence of *in situ* NH_3 doping on the dielectric was explored with the C–V test. A metal, a gate dielectric (Al_2O_3, AlON, AlNO) and Si form a metal–oxide–semiconductor (MOS) capacitor structure. The C–V curves of MOS capacitors measured at 1 MHz are shown in Fig. 3(a). For the gate dielectrics Al_2O_3, AlON and AlNO, the MOS oxide capacitances per unit area (C_{ox}) are 0.337 μF/cm^2, 0.381 μF/cm^2, and 0.357 μF/cm^2, respectively. C_{ox} is increased by the use of NH_3 doping, indicating improvement of the gate control capability. Figure 3(b) shows the k values of the three dielectrics and capacitance equivalent thicknesses. Based on $k = (C_{ox}t_{ox})/\varepsilon$, in which ε is the vacuum permittivity and t_{ox} is the thickness of the gate dielectric, the k values for Al_2O_3, AlON and AlNO are 7.6, 8.6, and 8.1, respectively. It is found that NH_3 doping can improve the k value of the dielectric layer due to the incorporation of nitrogen. Meanwhile, the capacitance equivalent thicknesses are decreased, which is conducive to a reduction of device size without affecting the gate control ability. Figure 3(c) shows the gate leakage current under gate voltages from −1 V to 1 V. After NH_3 doping, the dielectric leakage current decreases and the leakage current of AlON is one order of magnitude lower than that of Al_2O_3. From the electrical characterization, it is obvious that various electrical parameters are improved after NH_3 is doped into Al_2O_3. This

is mainly because NH_3 doping reduces the defects caused by oxygen vacancies.[28] However, the degree to which vacancies are suppressed is dependent on the sequence of NH_3 doping. When the film grows not as AlNO but as AlON, a better gate dielectric is obtained. An explanation for this is that the NH_3 doping sequence affects the bonding state of elements during the ALD process.

The surface roughness of the gate dielectric reflects the quality of the film. The roughness can affect the surface roughness scattering and thus the mobility of the carriers.[29,30] In this work, AFM is used to evaluate the root-mean square (RMS) roughness of the samples, as shown in Figs. 4(a)–4(c). The RMS roughness of Al_2O_3, AlON and AlNO is 0.217 nm, 0.169 nm, and 0.192 nm, respectively. Compared with the control sample Al_2O_3, samples with NH_3 doping have smaller RMS roughness. The AlON film has the best surface with the smallest surface roughness. This is consistent with the previous assumption that NH_3 doping and the sequence of doping have an impact on the quality of the dielectric layer. The flat surface is beneficial to improving the mobility of the carriers.[31]

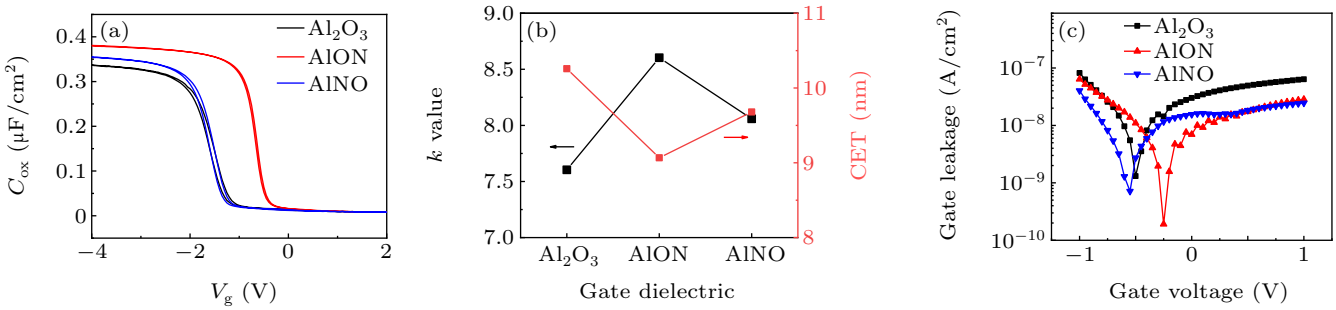


Fig. 3. (a) The C–V curves of MOS capacitors. (b) Relevant k values and capacitance equivalent thicknesses. (c) Gate leakage current (J_g)–V_g characteristics.

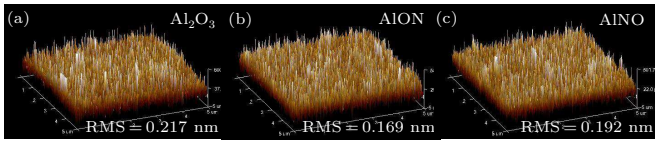


Fig. 4. AFM height image (5 μm × 5 μm) of the surface of the gate dielectric: (a) Al_2O_3, (b) AlON, (c) AlNO.

To further clarify the mechanism of NH_3 doping, XPS was used to analyze the chemical bonds of the three samples. In Fig. 5, O 1s has various binding energies of common chemical states, among which the low binding energy (531.2 eV) corresponds to lattice oxygen derived from O–Al in Al_2O_3 and non-lattice and surface oxygen have a higher binding energy (532.5 eV).[32] As shown in Figs. 5(a)–5(c), the red line represents lattice oxygen and the blue line represents non-lattice oxygen. The ratio of O-Al/O_{defect} in the film is reflected by the spectral peak intensity ratio and is 2.59, 4.42, and 3.91 in Al_2O_3, AlON and AlNO, respectively. Compared with the control sample Al_2O_3, the dielectric layers doped by NH_3 have a larger peak intensity ratio, representing the fewer oxygen vacancy defects which are repaired by nitrogen.

The XPS Al 2p spectra was extracted to analyze the bonding states of nitrogen and aluminum. As presented in Fig. 5(d), there is only one spectral peak derived from the Al–O bond at 74.55 eV in the Al_2O_3 dielectric layer. After the NH_3 doping, the peak of Al–N is visible at 73.31 eV, which indicates that nitrogen has been incorporated into Al_2O_3 and formed Al–N bonds. The peak intensity of Al–N represents the number of bonds formed and the peak intensity in the AlON layer is stronger than that in the AlNO layer, which is shown in Figs. 5(e) and 5(f). Corresponding to the peak intensity ratio in Figs. 5(b) and 5(c), there are more Al–N bonds in AlON, which means that more vacancies are repaired. These results show the influence of different nitrogen doping sequences on the dielectric.

Furthermore, the electrical characteristics of MoS_2 FETs were measured to study the effect of NH_3 doping on device performance. Figure 6(a) shows the output characteristics of the three samples, and the scanning gate voltage ranges from −2 V to 4 V in steps of 2 V. The samples with NH_3 doping achieve a higher drain current and the device has the highest drain current (8.0 μA/μm) at $V_g = 4$ V with AlON as the dielectric layer. Due to the effect of NH_3 doping on the repair of oxygen vacancies, carrier scattering at the interface of the channel and the dielectric layer is reduced, resulting in higher carrier transport efficiency and a larger current.

Figure 6(b) shows the transfer characteristics of the three samples with normalized drain current in order to avoid the influence of channel width on the output current. The threshold voltages V_{th} extracted in Fig. 6(b) are −0.74 V, −0.12 V, and −0.4 V for the samples with Al_2O_3, AlON and AlNO gate dielectric layers. It is obvious that the V_{th} of a MoS_2 FET has a positive drift with a NH_3-doped dielectric. Using Al_2O_3 as the dielectric layer, a mass of oxygen vacancies with positive charges exist in the film, causing negative V_{th}.[33] After NH_3 doping into the high-κ layer, charge traps are repaired and V_{th} has a positive drift.[34] The sample with AlON has the smallest $|V_{th}|$, which also indicates that the MoS_2/AlON interface has the fewest defective states.

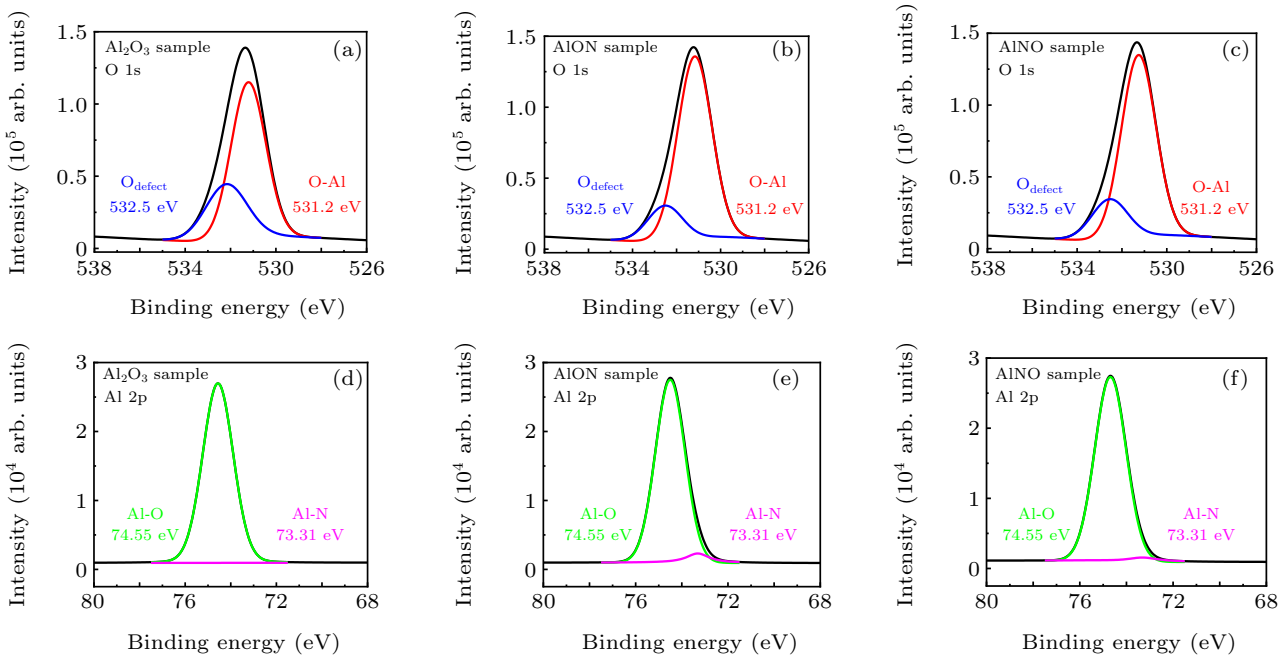


Fig. 5. Deconvolution of XPS O 1s and Al 2p spectra of the three samples.

Figure 6(c) demonstrates the transfer characteristics in a semilog scale with $V_{ds} = 0.2$ V, from which I_{on}/I_{off} can be extracted to be 1.33×10^5, 3.56×10^6, and 1.06×10^6 for samples with Al_2O_3, AlON and AlNO, respectively. The I_{on}/I_{off} of the sample with NH_3 doping is one order of magnitude larger than the sample without NH_3 doping. According to the above analysis, the repair of oxygen vacancy defects is helpful to reduce the carrier scattering capability, which can increase I_{on} and decrease I_{off} of transistors. From Fig. 6(c), the value of subthreshold swing (SS) can also be extracted; it is 139 mV/dec, 105 mV/dec, and 117 mV/dec for samples with Al_2O_3, AlON and AlNO, respectively. The sample with an AlON dielectric has the smallest SS, which is due to improvement of the interface quality after NH_3 doping.

In order to explore the carrier mobility trend of the device channel, decades of devices using Al_2O_3, AlON and AlNO as the gate dielectric are selected and the value is calculated by using the following equation:

$$\mu = \frac{1}{C_{ox}} \frac{L}{W} \frac{1}{V_{ds}} \frac{\Delta I_{ds}}{\Delta V_{gs}} \tag{1}$$

in which C_{ox} is the oxide capacitance per unit area of the gate dielectric, L and W are the channel length and width, respectively, and $\Delta I_{ds}/\Delta V_{gs}$ is the slope of the transfer characteristic curve on a linear scale. As shown in Fig. 6(d), it is obvious that the MoS_2 FETs with NH_3-doped Al_2O_3 have a higher carrier mobility.

In the process of Al_2O_3 deposition it is inevitable that oxygen vacancies will be generated because of the low crystallization temperature of Al_2O_3.[35] The existence of vacancies tends to form charge centers, and thus the charge scattering effect of the dielectric layer is affected. By doping nitrogen into the dielectric layer, oxygen vacancies are substituted by nitrogen atoms, which effectively screen the CI scattering in the dielectric layer and the k value of the dielectric is increased. In addition, the introduction of NH_3 during ALD growth of Al_2O_3 can also reduce the interface roughness of dielectric and channel materials, drastically decreasing the effect of interface scattering on channel carrier transport.

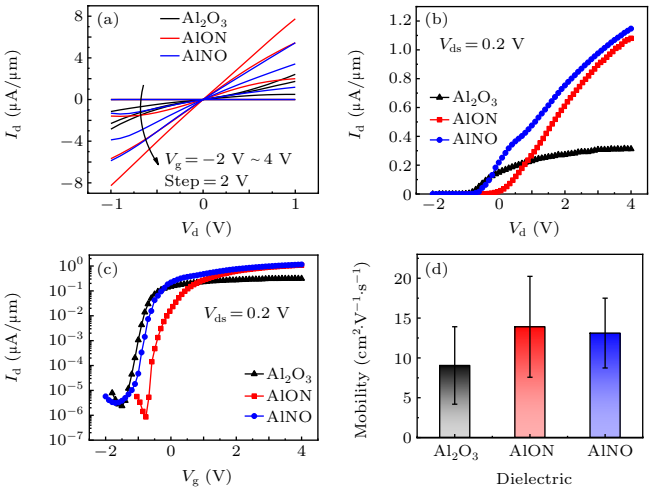


Fig. 6. (a) The I_d–V_{ds} curves in the linear region for the three samples. (b) Transfer characteristics of the three samples on a linear scale with $V_{ds} = 0.2$ V. (c) Transfer characteristics of the three samples on a semilog scale with $V_{ds} = 0.2$ V. (d) Average value of mobility of the three samples.

Figure 7 shows the off-state current and subthreshold swings of MoS_2 transistors produced using different treatment methods. Compared with other processes, the device in our work exhibits better performance and achieves a smaller SS (105 mV/dec) while maintaining a low off-state current.

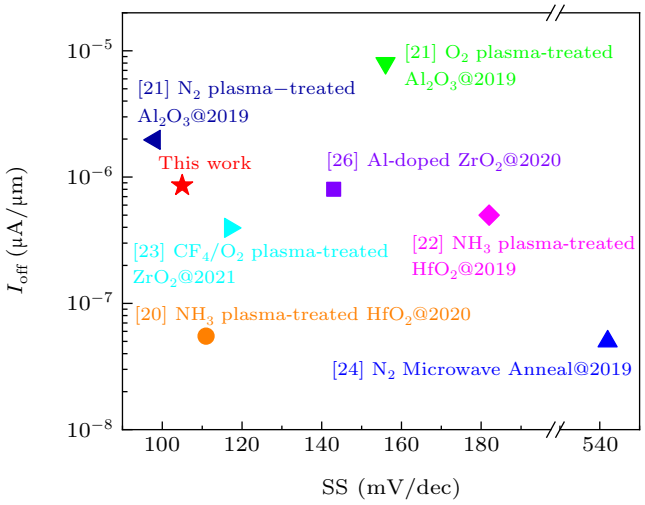


Fig. 7. A plot of off-state current versus the subthreshold swings from this work compared with MoS_2 FETs treated with other reported processes.

4. Conclusion

In summary, the processing method and the impacts of NH_3 *in situ* doping into an Al_2O_3 gate dielectric on MoS_2 FETs have been systematically investigated. Two different doping sequences were investigated in experiments. Through XPS and AFM characterization and the MOS capacitor electrical test, it was found that final doping of NH_3 during the ALD growth cycles demonstrates the best results. The oxygen vacancy defects in the Al_2O_3 dielectric are repaired by this *in situ* NH_3 doping, and the carrier scattering of the interfaces between the gate dielectric and TMD channel material is obviously reduced. As a result, the performance of the MoS_2 FET is effectively improved, and the threshold voltage shift to an ideal state close to 0 V. The *in situ* dielectric treatment reported in this paper provides an effective and simple method to improve performance as well as the threshold control in the development of future TMD integrated circuits.

Acknowledgments

Project supported by the National Natural Science Foundation of China (Grant Nos. 61774168 and 11764008) and the Opening Project of Key Laboratory of Microelectronic Devices & Integrated Technology, Institute of Microelectronics, Chinese Academy of Sciences.

References

[1] Novoselov K S, Geim A K, Morozov S V, Jiang D, Zhang Y, Dubonos S V, Grigorieva I V and Firsov A A 2004 *Science* **306** 666
[2] Bolotin K I, Sikes K J, Jiang Z, Klima M, Fudenberg G, Hone J, Kim P and Stormer H L 2008 *Solid State Commun.* **146** 351
[3] Desai S B, Madhvapathy S R, Sachid A B, Llinas J P, Wang Q, Ahn G H, Pitner G, Kim M J, Bokor J, Hu C, Wong H S P and Javey A 2016 *Science* **354** 99
[4] Luo K, Yang W, Pan Y, Yin H, Zhao C and Wu Z 2020 *J. Electron. Mater.* **49** 559
[5] Wang Q H, Kalantar-Zadeh K, Kis A, Coleman J N and Strano M S 2012 *Nat. Nanotechnol.* **7** 699
[6] Ma X, Fan Z, Wu J, Jiang X and Chen J 2018 *IEEE International Electron Devices Meeting*, December 1–5, 2018, San Francisco, USA, p. 24.2.1
[7] Mak K F, Lee C, Hone J, Shan J and Heinz T F 2010 *Phys. Rev. Lett.* **105** 136805
[8] Liu Y, Guo J, Zhu E, Liao L, Lee S, Ding M, Shakir I, Gambin V, Huang Y and Duan X 2018 *Nature* **557** 696
[9] Illarionov Y Y, Smithe K K H, Waltl M, Knobloch T, Pop E and Grasser T 2017 *IEEE Electron Dev. Lett.* **38** 1763
[10] Li W, Zhou J, Cai S, Yu Z, Zhang J, Fang N, Li T, Wu Y, Chen T, Xie X, Ma H, Yan K, Dai N, Wu X, Zhao H, Wang Z, He D, Pan L, Shi Y, Wang P, Chen W, Nagashio K, Duan X and Wang X 2019 *Nat. Electron.* **2** 563
[11] Cho B, Hahm M G, Choi M, Yoon J, Kim A R, Lee Y J, Park S G, Kwon J D, Kim C S, Song M, Jeong Y, Nam K S, Lee S, Yoo T J, Kang C G, Lee B H, Ko H C, Ajayan P M and Kim D H 2015 *Sci. Rep.* **5** 8052
[12] Koppens F H L, Mueller T, Avouris P, Ferrari A C, Vitiello M S and Polini M 2014 *Nat. Nanotechnol.* **9** 780
[13] Radisavljevic B, Whitwick M B and Kis A 2011 *ACS Nano* **5** 9934
[14] Kaasbjerg K, Thygesen K S and Jacobsen K W 2012 *Phys. Rev. B* **85** 115317
[15] Li Z, Xu J P, Liu L and Zhao X Y 2021 *Chin. Phys. B* **30** 018102
[16] Radisavljevic B, Radenovic A, Brivio J, Giacometti V and Kis A 2011 *Nat. Nanotechnol.* **6** 147
[17] Liu X, Cai Y and Liu Z J 2017 *Nanotechnology* **28** 164004
[18] Bolshakov P, Zhao P, Azcatl A, Hurley P K, Wallace R M and Young C D 2017 *Microelectron. Eng.* **178** 190
[19] Li X, Xiong X, Li T, Li S, Zhang Z and Wu Y 2017 *ACS Appl. Mater. Interfaces* **9** 44602
[20] Zhao X, Xu J, Liu L, Lai P T and Tang W M 2019 *IEEE Trans. Electron Dev.* **66** 4337
[21] Song X, Xu J, Liu L, Lai P T and Tang W M 2019 *Appl. Surf. Sci.* **481** 1028
[22] Chen J Y, Zhao X Y, Liu L and Xu J P 2019 *Chin. Phys. B* **28** 128101
[23] Song X, Xu J, Liu L and Lai P T 2021 *Appl. Surf. Sci.* **542** 148437
[24] Yang H, Li C, Yue L, Wen C, Zhang J and Wu D 2019 *IEEE Electron Device Lett.* **40** 1116
[25] Pan Y, Jia K, Huang K, Wu Z, Bai G, Yu J, Zhang Z, Zhang Q and Yin H 2019 *Nanotechnology* **30** 095202
[26] Song X, Xu J, Liu L, Deng Y, Lai P T and Tang W M 2020 *Nanotechnology* **31** 135206
[27] Kim J H, Park T J, Cho M, Jang J H, Seo M, Na K D, Hwang C S and Won J Y 2009 *J. Electrochem. Soc.* **156** G48
[28] Umezawa N, Shiraishi K, Ohno T, Watanabe H, Chikyow T, Torii K, Yamabe K, Yamada K, Kitajima H and Arikado T 2005 *Appl. Phys. Lett.* **86** 143507
[29] Touski S B and Hosseini M 2020 *Physica E* **116** 113763
[30] Ma X, Gong Y, Wu J, Li Y and Chen J 2019 *Jpn. J. Appl. Phys.* **58** 110905
[31] Song X, Xu J and Liu L 2020 *IEEE Trans. Electron Dev.* **67** 5196
[32] Lee H S, Park C S and Park H H 2014 *Appl. Phys. Lett.* **104** 191604
[33] Rai A, Valsaraj A, Movva H C P, Roy A, Ghosh R, Sonde S, Kang S, Chang J, Trivedi T, Dey R, Guchhait S, Larentis S, Register L F, Tutuc E and Banerjee S K 2015 *Nano Lett.* **15** 4329
[34] Deng L F, Lai P T, Chen W B, Xu J P, Liu Y R, Choi H W and Che C M 2011 *IEEE Electron Device Lett.* **32** 93
[35] Choi C H, Rhee S J, Jeon T S, Lu N, Sim J H, Clark R, Niwa M and Kwong D L 2002 *Digest. International Electron Devices Meeting*, December 8–11, 2002, San Francisco, USA, p. 857